USING THE TROJAN HORSE METHOD TO INVESTIGATE RESONANCES ABOVE AND BELOW THE THRESHOLD IN NUCLEAR REACTIONS OF ASTROPHYSICAL INTEREST*

M. La Cognata[a], C. Spitaleri[a,b], S. Cherubini[a,b], M. Gulino[a,c]
I. Indelicato[a,b], L. Lamia[b], R.G. Pizzone[a], S. Romano[a,b]
O. Trippella[d,e], A. Tumino[a,c]

[a]Laboratori Nazionali del Sud — INFN, Via S. Sofia 62, 95123 Catania, Italy
[b]Dipartimento di Fisica e Astronomia, University of Catania, Catania, Italy
[c]Kore University of Enna, Enna, Italy
[d]Dipartimento di Fisica, University of Perugia, Perugia, Italy
[e]Sezione INFN di Perugia, Perugia, Italy

(Received November 17, 2015)

Resonant reactions play an important role in astrophysics as they might significantly enhance the cross section with respect to the direct reaction contribution and alter the nucleosynthetic flow, namely, the predicted energy production and nucleosynthesis path. Moreover, resonances bear information about states in the intermediate compound nucleus formed in the reaction. Therefore, we have modified the Trojan horse method (THM) to investigate resonant reactions. In this work, we will discuss two examples of reactions of astrophysical interest, whose cross sections show a resonant behavior: the $^{19}\mathrm{F}(\alpha,n)^{16}\mathrm{O}$ cross section that displays resonances at energies above the particle emission threshold and the $^{13}\mathrm{C}(\alpha,n)^{16}\mathrm{O}$ reaction, dominated by the -3 keV sub-threshold resonance due to the 6.356 MeV level in $^{17}\mathrm{O}$.

DOI:10.5506/APhysPolB.47.681

1. General theory of THM in the case of resonant reactions

Resonant reactions play a key role in astrophysics as the appearance of resonances in the astrophysical factor might determine a dramatic change in the reaction rate, if resonances sit at energies of astrophysical interest. Therefore, resonances might determine a change in the nucleosynthetic flow

* Presented at the XXXIV Mazurian Lakes Conference on Physics, Piaski, Poland, September 6–13, 2015.

diverting it to unexpected paths and significantly changing the resulting isotopic abundance pattern. The occurrence of unexpected resonances or an inaccurate estimate of their strength might represent a severe issue in nuclear astrophysics as the access of energies of astrophysical interest is very difficult. As a consequence, not only indirect methods such as the Trojan horse method (THM) [1] were introduced in the past as complementary tools to direct approaches with the aim of reaching to the Gamow energy [2], but a special focus has been given to the treatment of resonant reactions.

A peculiar role is played by broad sub-threshold resonances. Even though the energy of a state of the compound system is lower than the entrance channel separation energy, making it impossible to excite such a state, if this is broad enough to have a tail extending to energies above the threshold, it can still be excited and potentially cause an increase of the astrophysical factor at almost vanishing energies. This interval is very critical as cross sections are extremely low, thus their measurement is very challenging, and the electron screening effect, also determining an exponential rise of the astrophysical factor at energies approaching zero, might conceal the contribution of such resonances. With this respect, the THM in its formulation for resonant reaction has proven an invaluable tool to investigate sub-threshold resonances and extract resonance parameters, including the corresponding asymptotic normalization coefficient.

Figure 1 describes a QF process occurring through the formation of a compound system F. In detail, following the QF breakup of a into its constituent clusters x–s, the participant fragment is captured by A, forming a quasi-bound system F later decaying to $b + B$, while the other cluster s is emitted without influencing neither the $A + x$ capture nor the following $F \to b + B$ decay. From the measurement of the energies and the angles of emissions of two out of three emitted particles, all the kinematic variables can be determined and, in particular, the x–A relative energy that is the most important variable for astrophysical application. Following [3, 4], under

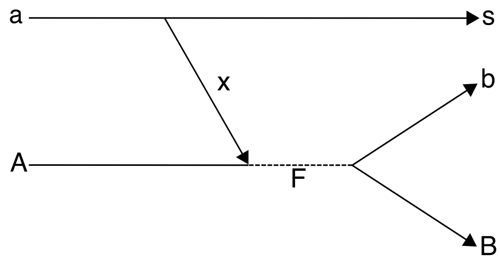

Fig. 1. The diagram describing the TH reaction $a + A \to b + B + s$ in the QF kinematics, proceeding through the formation of the $F = b + B$ resonant state.

the non-essential hypothesis that the nucleus a undergoing breakup is at rest in the laboratory system, the x–A relative energy can be written in terms of energy and momenta of the intervening particles

$$E_{x-A} = \frac{m_x}{m_x + m_A} E_A - \frac{p_s^2}{2\mu_{sF}} + \frac{\boldsymbol{p}_s \cdot \boldsymbol{p}_A}{m_x + m_A} - \varepsilon_{sx} \,, \tag{1}$$

where m_i, $\boldsymbol{p}_i$ and E_i are the mass, momentum and energy of the i^{th} particle, μ_{sF} the s–F reduced mass and ε_{sx} the x–s binding energy. Since part of the projectile energy is spent to break the impinging nucleus a and thanks to the x–s inter cluster motion, astrophysical energies can be achieved in the x–A channel of the TH reaction using beam energies of few tens of MeV, bypassing Coulomb barrier and the electron screening enhancement. Furthermore, negative E_{x-A} energies can be explored by choosing a suitable combination of beam energy, spectator momentum and target nucleus a. Indeed, in a number of cases the same participant x can be transferred off different targets a, each contributing to Eq. (1) with binding energy ε_{sx}.

Therefore, THM can be used to observe, with no need of extrapolation or correction for the electron screening enhancement, both resonances at astrophysical energies and lying close to the $F \to x + A$ threshold, which are of particular astrophysical interest. However, the $A(x,b)B$ sub-reaction is half-off-energy-shell (HOES) as fragments b and B in the exit channel are real, while particle x is virtual, namely, the mass-shell equation is not satisfied for it. Since astrophysical factors obtained using direct approaches are on-energy-shell (OES) as particles in the entrance and exit channels are all real, the HOES astrophysical factor cannot be right juxtaposed to the direct one. This reason and the need of a theory specifically developed to deal with multi resonance reactions has urged us to improve the theoretical treatment of THM, leading to a new general theory based on DWBA and post continuum discretized coupled channels (CDCC) formalism, the surface integral formulation of the reaction theory, and the R-matrix method [3, 5]. In what follows, we give a short summary of the main equations necessary to link the cross section of the TH reaction $a + A \to b + B + s$ to the one of astrophysical interest, $A(x,b)B$, in the case of a resonant process.

Starting with the plane wave approximation (PWA) in the prior form and neglecting, for simplicity, the spins of the particles involved in the reaction, the amplitude of the $a + A \to b + B + s$ takes the form

$$M^{\text{PWA(prior)}}(P, \boldsymbol{k}_{aA}) = \left\langle \chi_{sF}^{(0)} \varPsi_{bB}^{(-)} | V_{xA} | \varphi_a \varphi_A \chi_{aA}^{(0)} \right\rangle \,, \tag{2}$$

where $P = (\boldsymbol{k}_{sF},\, \boldsymbol{k}_{bB})$ is the six-dimensional momentum describing the three-body system s, b and B. $\chi_{aA}^{(0)} = \exp\left(i\boldsymbol{k}_{aA} \cdot \boldsymbol{r}_{aA}\right)$, $\chi_{sF}^{(0)} = \exp\left(i\boldsymbol{k}_{sF} \cdot \boldsymbol{r}_{sF}\right)$,

$\boldsymbol{r}_{ij}$ and $\boldsymbol{k}_{ij}$ are the relative coordinate and relative momentum of nuclei i and j, $\Psi_{bB}^{(-)}$ is the wave function of the fragments b and B in the exit channel, $F = b + B$, V_{xA} is the interaction potential of x and the target nucleus A, φ_a and φ_A are the bound state wave function of nuclei a and A, respectively. In the development of the theory, the prior form looks more preferable than the post-form because it does not contain the interaction potential of the exiting particle s, allowing us to treat it as a spectator. If we assume that resonant reaction mechanism is dominant in the explored energy region, the wave function $\Psi_{bB}^{(-)}$ can be conveniently expressed using the spectral decomposition given by Eq. (3.8.1) of [6]. This leads to the shell-model based resonant R-matrix representation for $\Psi_{bB}^{(-)}$ which is similar to the level decomposition for the wave function in the internal region in the R-matrix approach

$$\Psi_{bB}^{(-)} \approx \sum_{\nu,\tau=1}^{N} \tilde{V}_{\nu\, bB}(E_{bB}) \left[\boldsymbol{A}^{-1}\right]_{\nu\tau} \Psi_{\tau} \,. \tag{3}$$

Here, N is the number of the levels included, E_{bB} is the relative kinetic energy of nuclei in the channel $b + B$, Ψ_τ is the bound state wave function describing the compound system F excited to the level τ. $\boldsymbol{A}_{\nu\tau}$ is the same level matrix as in the conventional R-matrix theory and is given by Eq. (4.2.20b) of [6]. Therefore, it depends on the entry and exit channels reduced width amplitudes, energy levels and energy shifts. It means that reduced width amplitudes and level energies can be obtained from the fitting of the experimental THM cross section and used to deduce the $A(x, b)B$ astrophysical factor, since they are the same in both THM and direct data. HOES effects can affect the phases determining interference effects and the relative heights of the resonances, as it will be shown later, but the reduced widths γ, containing the nuclear structure effects, appear in the same way in THM and direct data.

In Eq. (3), $\tilde{V}_{\nu\, bB}(E_{bB})$ is the resonant form factor for the decay of the resonance level ν described by the compound state Ψ_ν into the channel $\alpha = bB$

$$\tilde{V}_{\nu\,\alpha}(E_\alpha) = \left\langle \chi_\alpha^{(-)}\, \varphi_\alpha | \Delta V_\alpha | \Psi_\nu \right\rangle \,, \tag{4}$$

strictly linked to the R-matrix formal partial resonance width for the decay of this level into the channel α, given by

$$\tilde{\Gamma}_{\nu\,\alpha}(E_\alpha) = 2\,\pi \left| \tilde{V}_{\nu\,\alpha}(E_\alpha) \right|^2 \,. \tag{5}$$

Introducing Eq. (3) into Eq. (2), taking into account spins of the interacting particles, considering only the s-wave bound state $a = s + x$ and neglecting the internal degrees of freedom of the transferred particle x, we get the prior PWA amplitude of the THM cross section takes the form [3]

$$
\begin{aligned}
& M^{\mathrm{PWA(prior)}}(P,\boldsymbol{k}_{aA}) = (2\pi)^2\sqrt{\frac{1}{\mu_{bB}k_{bB}}}\varphi_a(\boldsymbol{p}_{sx}) \\
& \times \sum_{J_F M_F j' l l' m_{j'} m_l m_{l'} M_x} i^{l+l'} \left\langle j m_j l m_l | J_F M_F \right\rangle \left\langle j' m_{j'} l' m_{l'} | J_F M_F \right\rangle \\
& \times \left\langle J_x M_x J_A M_A | j' m_{j'} \right\rangle \left\langle J_s M_s J_x M_x | J_a M_a \right\rangle \\
& \times \exp\left[-i\delta^{hs}_{bB\,l}\right] Y_{l m_l}\left(-\hat{\boldsymbol{k}}_{bB}\right) \sum_{\nu\tau=1}^{N} \left[\Gamma_{\nu bBjlJ_F}\right]^{1/2} \left[\boldsymbol{A}^{-1}\right]_{\nu\tau} Y^{*}_{l'm'}(\hat{\boldsymbol{p}}_{xA}) \\
& \times \sqrt{\frac{R_{xA}}{\mu_{xA}}}\left[\Gamma_{\nu xAl'j'J_F}(E_{xA})\right]^{1/2} P_{l'}^{-1/2}(k_{xA},R_{xA}) \\
& \times \Big(j_{l'}(p_{xA}R_{xA})\left[(B_{xA\,l'}(k_{xA},R_{xA})-1)-D_{xA\,l'}(p_{xA},R_{xA})\right] \\
& + 2Z_xZ_Ae^2\mu_{xA}\int_{R_{xA}}^{\infty}\mathrm{d}r_{xA}\frac{O_{l'}(k_{xA},r_{xA})}{O_{l'}(k_{xA},R_{xA})}j_{l'}(p_{xA}r_{xA})\Big)\,.
\end{aligned}
\tag{6}
$$

Here, $\boldsymbol{p}_{ij}$ is the i–j relative momentum in the case of off-energy-shell particles, thus $E_{ij} \neq p_{ij}^2/2\mu_{ij}$ (while $\boldsymbol{k}_{ij}$ is calculated assuming the particles on-shell), $\delta^{hs}_{bB\,l}$ is the solid sphere scattering phase shift, R_{xA} the $x+A$ channel radius,

$$
B_{xA\,l'}(k_{xA},R_{xA}) = R_{xA}\frac{\left.\frac{\partial O_{l'}(k_{xA},R_{xA})}{\partial r_{xA}}\right|_{r_{xA}=R_{xA}}}{O_{l'}(k_{xA},R_{xA})}
\tag{7}
$$

is the logarithmic derivative as in the R-matrix method,

$$
O_{l'}(k_{xA},R_{xA}) = \sqrt{\frac{k_{xA}R_{xA}}{P_{l'}(k_{xA},R_{xA})}}\exp\left[-i\delta^{hs}_{xA\,l'}\right]
\tag{8}
$$

is the outgoing spherical wave, $P_{l'}(k_{xA},R_{xA})$ the l'-wave penetrability factor,

$$
D_{xA\,l'}(p_{xA},R_{xA}) = R_{xA}\frac{\left.\frac{\partial j_{l'}(p_{xA},R_{xA})}{\partial r_{xA}}\right|_{r_{xA}=R_{xA}}}{j_{l'}(p_{xA},R_{xA})}
\tag{9}
$$

the logarithmic derivative and $j_{l'}(p_{xA},R_{xA})$ the spherical Bessel function, N the number of the levels included. This is a generalization of the R-matrix approach because we consider reactions with three particles in the exit channel, where the TH-nucleus a in the initial states carries the transferred particle x, which is off-energy-shell. It allows one to treat both multi-level (interfering) and single-level two-channel cases (non-interfering resonances). Even though a simple PWA is used here, the a–A and the s–F interactions can be treated as well within the distorted waves (DWBA) or the more advanced CDCC formalism [5]. This is very important as it opens the possibility to make normalization to direct data, at present a major drawback of THM especially in the investigation of reactions induced by radioactive ion beams, where direct data might be of poor quality or even absent.

As one can see from Eq. (6), the presence of the factor $P_{l'}^{-1/2}(k_{xA}, R_{xA})$ eliminates the penetrability factor in the $x + A$ channel, which is the entry channel of the binary sub-reaction. The compensation of the penetrability factor in this entry channel is the main advantage of the THM, which allows one to measure the astrophysical factor of the binary reaction down to zero E_{xA} energy. Moreover, resonances that can be populated with large l only are not suppressed, thus they can be observable even in the case they are not in direct measurements, making the THM a powerful spectroscopic tool as well.

In the case of sub-threshold resonances, the equations above have to be modified as for bound states at negative energies penetrability is zero, but the shift function appearing in R-matrix formula [7] can still be defined as the logarithmic derivative of the Whittaker function [8]. If $\varphi(r)$ is the single-channel bound state wave function, the R-matrix eigenfunction $w(r)$ is proportional to $\varphi(r)$ inside the R-matrix radius a: $\varphi(r) = Aw(r)$, where $A^2 = 1 - \int_a^\infty |\varphi(r)|^2 dr$ reflects the different normalization requirements. Outside the R-matrix radius, the Whittaker function $W(r)$ describes the asymptotic behavior of the bound state wave function of two charged particles, the asymptotic normalization coefficient (ANC) defining the amplitude of its tail, namely, the ANC value C is the coefficient in $\varphi(r) = CW(r)$ for the Whittaker function [9, 10]. The reduced width is therefore [8]

$$\gamma^2 = \frac{\hbar^2}{2\mu a} \frac{C^2 W(a)^2}{1 - C^2 \int_a^\infty |W(r)|^2 dr} \,. \tag{10}$$

Thus, from the THM measurement of a sub-threshold state, yielding the reduced widths γ, the ANC can be deduced, clearly disclosing the deep connection of the two indirect approaches [4, 11].

1.1. Investigation of resonances above the threshold: the $^{19}F(p,\alpha)^{16}O$ reaction

The s-process is a major nucleosynthesis scenario, responsible for the production of a large fraction of nuclei heavier than iron [2, 12]. Asymptotic giant branch (AGB) stars [13] are a class of red giants, alternately burning hydrogen and helium in shell and responsible for the production of the main component of s-process nuclei, through slow neutron captures on seed nuclei [14]. AGB stars are also regarded as the main fluorine contributors to the Galactic supply [15, 16], fluorine nucleosynthesis taking place in the same environment where s-nuclei are forged. Since fluorine abundance is very sensitive to the physical conditions and mixing phenomena taking place in the inner layers of AGB stars [17], it might represent a strong constraint of stellar internal structure. Therefore, understanding of fluorine production may lead to a more accurate picture of heavy element nucleosynthesis. The $^{19}\mathrm{F}(p,\alpha)^{16}\mathrm{O}$ channel is the main fluorine depleting reaction in hydrogen rich environments, such as the outer layers of AGB stars, where fluorine can experience temperatures large enough to determine its destruction, owing to extra-mixing processes [17].

Only one set of direct data is available [18] on the $^{19}\mathrm{F}(p,\alpha)^{16}\mathrm{O}$ astrophysical factor at the energies $\mathrm{E_{cm}} \leq 300$ keV, where fluorine burning is most effective (Gamow energy [12]), in particular for the α_0 channel, corresponding to the emission of α-particles off $^{20}\mathrm{Ne}$ leaving $^{16}\mathrm{O}$ in its ground state. This is regarded as the main contribution to the $^{19}\mathrm{F}(p,\alpha)^{16}\mathrm{O}$ astrophysical factor [19]. Widely adopted compilations such as the Nuclear Astrophysics Compilation of Reaction Rates (NACRE) [20] used data from different sources to supply a recommended astrophysical factor and, consequently, reaction rate. However, the lowest energy data reach 461 keV center-of-mass energy [21], well above the Gamow peak, and only the unpublished data of [22] partially cover the range of astrophysical relevance. While the older measurement discussed in [21] indicates the existence of two resonances with $J^\pi = 1^-$ and 0^+ at $E_{\mathrm{cm}} \sim 0.4$ MeV, the unpublished data of [22] and the NACRE extrapolation support a non-resonant trend of the low-energy $S(E)$-factor. This contradiction and the very simple recommended extrapolation to astrophysical energies have generated speculations about a nuclear origin of the discrepancies observed in Galactic fluorine studies [23], since the largest observed fluorine overabundances cannot be explained with standard AGB models including extra mixing (see [24], for instance). This has requested a reassessment of the nuclear reaction rates involved in fluorine production and destruction.

Since the astrophysical factor shows a definitely resonant behavior above 0.6 MeV, the THM in its modified version developed to handle resonant reactions is very suited to investigate the $^{19}\mathrm{F}(p,\alpha)^{16}\mathrm{O}$ astrophysical factor aiming at disclosing the occurrence of resonances at astrophysical energies as well. To this purpose, the QF $^{2}\mathrm{H}(^{19}\mathrm{F},\alpha^{16}\mathrm{O})n$ reaction at 50 MeV beam energy was measured by means of a 1-mm collimated $^{19}\mathrm{F}$ beam impinging onto deuterated polyethylene (CD2) targets ($\sim 100\,\mu\mathrm{g\,cm^{-2}}$ thick). Therefore, we used deuterons to transfer protons and induce the $^{19}\mathrm{F}(p,\alpha)^{16}\mathrm{O}$ QF reaction. More details on the experimental setup and the analysis procedures are given in [23]. Here, we underscore that by using Eq. (6) we derived the resonance reduced widths of a number of resonances and, in particular, of a 113 keV peak sitting inside the Gamow window, which was not observed before and might have important consequences for astrophysics. The p–^{19}F relative energy spectrum spanned an energy interval from 0 to about 1 MeV, making it possible to normalize the THM astrophysical factor to the existing direct data. In the original work [23], THM data were normalized to a weighed average of existing direct data, as reported in the NACRE compilation [20], in the energy window 0.6–0.8 MeV. Recently, new direct data were made available in the normalization energy region [25], calling for a reanalysis of THM results [26].

Figure 2 shows the $S(E)$-factor calculated with the resonance parameters from the fitting of THM data below 600 keV. Above this energy, the resonance parameters are taken from the fitting of the data from [25] for normalization. This is possible as in the modified R-matrix approach the same reduced widths appear as in the on-energy-shell $S(E)$-factor, the only difference being the absence of any Coulomb or centrifugal penetrability

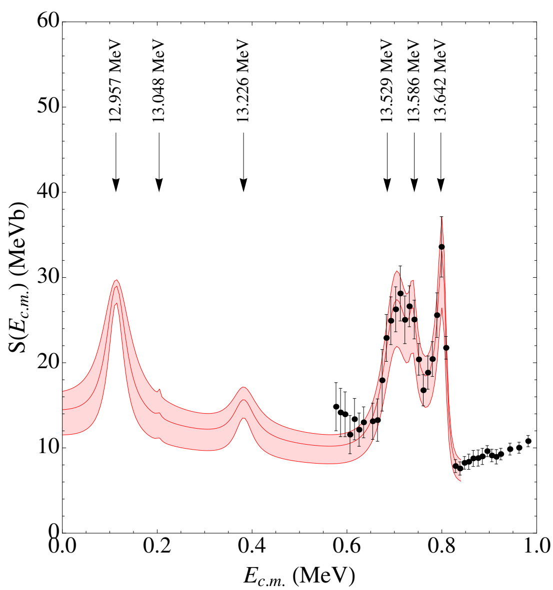

Fig. 2. (Color on-line) THM astrophysical factor of the ^{19}F$(p,\alpha_0)^{16}$O reaction, normalized to the data from [25] above 600 keV, as shown in [26]. The middle solid (red) line marks the recommended S-factor, while the upper and lower solid (red) lines stand for upper and lower limits set by combined statistical, normalization and energy shift error. The solid symbols represent the direct astrophysical factor in [25]. Finally, the arrows mark the ^{20}Ne states contributing to the $S(E)$-factor.

factor in the entrance channel. Since the TH cross section yielded the resonance contribution only, the non-resonant part of the cross section was taken from [20]. The middle solid (red) curve marks the $S(E)$-factor computed using the parameters from the best fit, while the gray (red) band arises from the uncertainties on the resonance parameters, due to the combined statistical, normalization and energy shift error (including correlation). An average error of 20% is obtained. This is different from the result in [23], where only the errors affecting the resonances below 600 keV were reported (no correlations). At present, the main source of uncertainty is due to the non-resonant contribution to the astrophysical factor, since the one given in [20] is based on a very simple calculation. New direct measurements are of utmost importance to have a more realistic non-resonant contribution at low energies.

1.2. The sub-threshold resonance case: the $^{13}C(\alpha,n)^{16}O$ reaction

A key reaction for the understanding of the s-process is the $^{13}\mathrm{C}(\alpha,n)^{16}\mathrm{O}$ process. In AGB stars, protons from the outer layers are mixed downward to the base of the convective envelope, following the quenching of the H-burning shell. Some protons are injected into the intershell region and are quickly captured by carbon nuclei, eventually leading to the formation of a $^{13}\mathrm{C}$ pocket [27]. Then, $^{13}\mathrm{C}$ nuclei give up their excess neutrons to heavier nuclei through the $^{13}\mathrm{C}(\alpha,n)^{16}\mathrm{O}$ reaction, at temperatures varying between 0.8×10^8 K and 1×10^8 K [28]. The $^{13}\mathrm{C}(\alpha,n)^{16}\mathrm{O}$ reaction is then considered the neutron source of the main component of the s-process. At 0.9×10^8 K, the energy range where the $^{13}\mathrm{C}(\alpha,n)^{16}\mathrm{O}$ reaction is most effective, the Gamow window [12], is $\sim$ 140–230 keV. In such region, its direct measurement is exceedingly challenging because of the Coulomb barrier, exponentially suppressing the cross section, and the interplay between the -3 keV resonance and atomic electron screening [2]. Indeed, direct measurements have shown an enhancement of the astrophysical factor at energies approaching zero, owing to the 3 keV sub-threshold resonance determined by the population of the 6.356 MeV level in $^{17}\mathrm{O}$.

Direct measurements, indirect methods and theoretical calculations aimed at constraining the contribution of the 6.356 MeV $^{17}\mathrm{O}$ state to the astrophysical factor. Regarding direct measurements, the lowest energy reached is $\sim$ 280 keV [29]; lower energies cannot be reached with present-day facilities owing to the strong suppression of the cross section due to Coulomb penetration factor. Indeed, at $\sim$ 300 keV, the cross section of the $^{13}\mathrm{C}(\alpha,n)^{16}\mathrm{O}$ reaction is already as low as $\sim 10^{-10}$ b. Moreover, at this energy, the astrophysical factor has to be corrected for atomic electron screening of the nuclear charges [2]; since our current understanding of the electron screening effect is rather incomplete, correcting the low-energy trend of the S-factor might result in systematic errors. Therefore, extrapolation is necessary at present to assess the astrophysical factor of the ^{13}C$(\alpha,n)^{16}$O reaction at astrophysical energy. Extrapolation has been performed mostly using the R-matrix approach [7]; the most recent result [30], employing a broad data set including renormalized ^{13}C$(\alpha,n)^{16}$O astrophysical factors reports a 100 keV astrophysical factor $S(100\text{ keV}) = 3.3^{+1.8}_{-1.4} \times 10^6$ MeV b. Indirect measurements aim at deducing the ANC or the spectroscopic factor of the 6.356 MeV level in ^{17}O through α-transfer reactions (see [4] for a review of the indirect measurements). However, contradicting values of the ANC or of the spectroscopic factors were obtained. Moreover, systematic errors might be introduced, especially in the case of the extraction of the spectroscopic factor, because of possible background or ambiguities in optical potential parameters used in the calculations. Theoretical calculations were also performed [31, 32], in fair agreement with extrapolated S-factors taking into account uncertainties on the data and on the calculations. To sum up, an untenable spread in the values of the low-energy S-factor is present, ranging from 1.2×10^6 [33] to 6.3×10^6 MeV b [34] at a reference center-of-mass energy of 100 keV.

The THM is well-suited to investigate the ^{13}C$(\alpha,n)^{16}$O process, as it allows us to explore the negative energy region and, consequently, to observe the -3 keV peak. The experiment was performed at the John D. Fox Superconducting Linear Accelerator Facility at Florida State University, which delivered a 7.82 MeV, 1 mm spot ^{6}Li beam impinging onto a 53 μg/cm^2, 99% ^{13}C enriched foil. Therefore, we used ^{6}Li, having a well-known $\alpha + d$ structure, to transfer an α-particle to ^{13}C while d was emitted without interacting in QF kinematics. ^{16}O from the ^{13}C$(\alpha,n)^{16}$O sub-reaction and deuterons were detected, to maximize the detection efficiency and reduce systematic uncertainties.

Figure 3 shows the THM S-factor (squared/red band), compared with direct data in the literature (black symbols). The blue line demonstrates how the S-factor would look like in the case the -3 keV peak is not present. More details on the figure are given in Ref. [4]. The THM S-factor is obtained by taking the resonance reduced widths from the THM cross section of the ^{13}C$(^6$Li$, n^{16}$O$)^2$H QF process, fitted using Eq. (6). This is possible as in the modified R-matrix approach the same reduced widths appear as in the OES $S(E)$-factor, the difference being the absence of any Coulomb or centrifugal penetration factor in the entrance channel and of the electron screening effect. Normalization was obtained by scaling the resonance parameters to those of the peaks above ~ 500 keV. The THM astrophysical factor agrees, within uncertainties, with existing extrapolations of the ^{13}C$(\alpha,n)^{16}$O S-factor to the Gamow window, with theoretical calculations and other indirect approaches, taking into account the mentioned possible

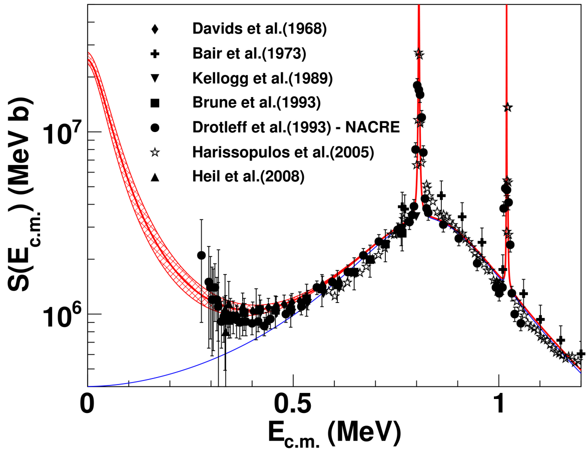

Fig. 3. (Color on-line) R-matrix calculated $S(E)$-factor of the ${}^{13}\mathrm{C}(\alpha,n){}^{16}\mathrm{O}$ reaction (red band), obtained using the THM resonance parameters below $E_{\mathrm{cm}} = 500$ keV and the [30] parameters above, from Ref. [4]. The upper and lower (red) lines delimiting the band mark the range allowed by experimental errors affecting THM data and by the normalization uncertainty. The R-matrix $S(E)$-factor not including the sub-threshold resonance at -3 keV is displayed by the solid (blue) line. Black symbols are used for direct data normalized as in [30]. Different marks are used for each data set, as specified in the inset. See Ref. [4] for more details.

sources of systematic errors. The THM results, however, seem to indicate that the largest values of the extrapolated S-factor are preferable and should be used in astrophysical calculations. Indeed, the recommended THM S-factor at $\mathrm{E}_{\mathrm{cm}} = 100$ keV is $5.3 \pm 0.9 \times 10^6$ MeV b, about 40% larger than the value provided by [30]. The most striking result is a significant reduction of the uncertainty affecting the ${}^{13}\mathrm{C}(\alpha,n){}^{16}\mathrm{O}$ S-factor at the Gamow peak, which is reduced from about 50% to about 20%. This is possible as the -3 keV peak is accessible using the THM approach as modified to handle resonant reactions, as an essentially background free indirect measurement was performed and because sources of systematic errors, related to normalization or to the adopted theoretical framework, have been addressed in the data analysis.

REFERENCES

[1] C. Spitaleri, Proc. of the 5$^{\mathrm{th}}$ Winter School on Hadronic Physics: Problems of Fundamental Modern Physics II, Eds. R. Cherubini, P. Dalpiaz, B. Minetti, World Scientific, Singapore, 1991, pp. 21–36.

[2] C.E. Rolfs, W.S. Rodney, *Cauldrons in the Cosmos*, University of Chicago Press, Chicago 1988.

[3] R.E. Tribble *et al.*, *Rep. Prog. Phys.* **77**, 106901 (2014).

[4] M. La Cognata *et al.*, *Astrophys. J.* **777**, 143 (2013).

[5] A.M. Mukhamedzhanov, *Phys. Rev. C* **83**, 044604 (2011).

[6] C. Mahaux, H.A. Weidenmüller, *Shell-Model Approach to Nuclear Reactions*, North-Holland Publishing Company, Amsterdam 1969.

[7] A.M. Lane, R.G. Thomas, *Rev. Mod. Phys.* **30**, 257 (1958).

[8] I.J. Thompson, F.M. Nunes, *Nuclear Reactions for Astrophysics: Principles, Calculation and Applications of Low-Energy Reactions*, Cambridge University Press, Cambridge 2009.

[9] A.M. Mukhamedzhanov, N.K. Timofeyuk, R.E. Tribble, *Phys. Rev. C* **51**, 3472 (1995).

[10] A.M. Mukhamedzhanov, R.E. Tribble, *Phys. Rev. C* **59**, 3418 (1999).

[11] M. La Cognata *et al.*, *Phys. Rev. Lett.* **109**, 232701 (2012).

[12] C. Iliadis, *Nuclear Physics of Stars*, Wiley-VCH Verlag, 2007.

[13] B.S. Meyer, *Annu. Rev. Astron. Astrophys.* **32**, 153 (1994).

[14] F. Käppeler *et al.*, *Rev. Mod. Phys.* **83**, 157 (2011).

[15] A. Jorissen *et al.*, *Astron. Astrophys.* **261**, 164 (1992).

[16] S. Cristallo *et al.*, *Astrophys. J.* **696**, 797 (2009).

[17] M. Lugaro *et al.*, *Astrophys. J.* **615**, 934 (2004).

[18] I. Lombardo *et al.*, *Phys. Lett. B* **748**, 178 (2015).

[19] A. Spyrou *et al.*, *Eur. Phys. J. A* **7**, 79 (2000).

[20] C. Angulo *et al.*, *Nucl. Phys. A* **656**, 3 (1999).

[21] G. Breuer, *Z. Phys.* **154**, 339 (1959).

[22] H. Lorentz-Wirzba, Ph.D. Thesis, Universität Münster, 1978.

[23] M. La Cognata *et al.*, *Astrophys. J.* **739**, L54 (2011).

[24] S. Lucatello *et al.*, *Astrophys. J.* **729**, 40 (2011).

[25] I. Lombardo *et al.*, *J. Phys. G Nucl. Phys.* **40**, 125102 (2013).

[26] M. La Cognata *et al.*, *Astrophys. J.*, in press, 2011.

[27] R. Gallino *et al.*, *Astrophys. J.* **497**, 388 (1998).

[28] M. Busso, R. Gallino, G.J. Wasserburg, *Annu. Rev. Astron. Astrophys.* **37**, 239 (1999).

[29] H.W. Drotleff *et al.*, *Astrophys. J.* **414**, 735 (1993).

[30] M. Heil *et al.*, *Phys. Rev. C* **78**, 025803 (2008).

[31] P. Descouvemont, *Phys. Rev. C* **36**, 2206 (1987).

[32] M. Dufour, P. Descouvemont, *Phys. Rev. C* **72**, 015801 (2005).

[33] E.D. Johnson *et al.*, *Phys. Rev. Lett.* **97**, 192701 (2006).

[34] G.M. Hale, *Nucl. Phys. A* **621**, 177 (1997).